frontiers in Chemistry

ORIGINAL RESEARCH
published: 28 February 2020
doi: 10.3389/fchem.2020.00146

CO_2 Capture With Absorbents of Tertiary Amine Functionalized Nano–SiO_2

Nanjun Lai[1,2,3,4]*, **Qingru Zhu**[1,4], **Dongyu Qiao**[5], **Ke Chen**[6], **Lei Tang**[1,4], **Dongdong Wang**[1,4], **Wei He**[1], **Yuemei Chen**[1] **and Tong Yu**[1]

[1] School of Chemistry and Chemical Engineering, Southwest Petroleum University, Chengdu, China, [2] State Key Laboratory of Oil and Gas Geology and Exploitation, Chengdu University of Technology, Chengdu, China, [3] State Key Laboratory of Polymer Molecular Engineering, Fudan University, Shanghai, China, [4] Key Laboratory of Oilfield Chemistry (KLOC), CNPC, Beijing, China, [5] Engineer Technology Research Institute, CNPC Xibu Drilling Engineering Company Limited, Ürümqi, China, [6] China National Offshore Oil Corporation (CNOOC) Energy Development Company Limited, Tianjin, China

To improve CO_2 adsorption performance of nanoparticle absorbents, a novel tertiary amine functionalized nano–SiO_2 (NS–NR_2) was synthesized based on the 3–aminopropyltrimethoxysilane (KH540) modified nano–SiO_2 (NS–NH_2) via methylation. The chemical structure and performances of the NS–NR_2 were characterized through a series of experiments, which revealed that NS–NR_2 can react with CO_2 in water and nanofluid with low viscosity revealed better CO_2 capture. The CO_2 capture mechanism of NS–NR_2 was studied by kinetic models. From the correlation coefficient, the pseudo second order model was found to fit well with the experiment data. The influencing factors were investigated, including temperature, dispersants, and cycling numbers. Results has shown the additional surfactant to greatly promote the CO_2 adsorption performance of NS–NR_2 because of the better dispersity of nanoparticles. This work proved that NS–NR_2 yields low viscosity, high capacity for CO_2 capture, and good regenerability in water. NS–NR_2 with high CO_2 capture will play a role in storing CO_2 to enhanced oil recovery in CO_2 flooding.

Keywords: nano–SiO_2, tertiary amine, CO_2 capture, low viscosity, regenerability

Edited by:
Qing You,
China University of Geosciences, China

Reviewed by:
Helei Liu,
University of British Columbia, Canada
Guillermo Javier Copello,
National Council for Scientific and Technical Research (CONICET), Argentina

***Correspondence:**
Nanjun Lai
lainanjun@126.com

Specialty section:
This article was submitted to Nanoscience, a section of the journal Frontiers in Chemistry

Received: 11 November 2019
Accepted: 17 February 2020
Published: 28 February 2020

Citation:
Lai N, Zhu Q, Qiao D, Chen K, Tang L, Wang D, He W, Chen Y and Yu T (2020) CO_2 Capture With Absorbents of Tertiary Amine Functionalized Nano–SiO_2. Front. Chem. 8:146. doi: 10.3389/fchem.2020.00146

INTRODUCTION

In recent years, humans have been endangered by greenhouse effect leading to global warming. Carbon dioxide (CO_2) emission source from the burn of fossil fuels catches much attention because of it is a major factor to the greenhouse effect (Sarkodie and Strezov, 2019). One method to assuage the greenhouse effect is to capture CO_2 from emission sources and then save it in stratum or apply it for enhanced oil recovery in low permeability reservoirs. Therefore, a feasible approach called carbon capture and storage (CCS) technologies have developed, including membranes, cryogenic distillation, gas adsorption with liquids or solids, and others (Benson and Orr, 2011; Bui et al., 2018). However, membrane–based separation is not a suitable way for CO_2 capture because perfection wants to be made in the areas of CO_2 selectivity, permeability, cost, and performance depletion over time (all caused by a variety of factors). Moreover, because of the high energy costs involved, cryogenic distillation is not optimally suitable. Solvents and solid sorbents have been reported for CO_2 capture, such as basic solvents, supported amine, and ammonium materials, as the primary classes of chemical sorbents (Heydari-Gorji et al., 2011; Darunte et al., 2016; Hahn et al., 2016; Sanz-Perez et al., 2016; Kong et al., 2019). The adsorption of CO_2 by solvents is a commercially available method, but the regeneration process of the solvents is highly energy intensive and expensive (Rochelle, 2009). The adsorption of CO_2 by solid sorbents has recently attracted much attention in the study of CO_2 capture (Lee and Park, 2015).

Nano silica (SiO_2) solid sorbents have been investigated for CO_2 capture given their high pore volume, large surface, and ease of functionality (Liu et al., 2016; Lai et al., 2017, 2019; Wang et al., 2019). Jiao et al. (2015) prepared mesoporous silica (MSU–J) with a wormhole framework texture, the surface of MSU–J was modified with triethylenetetramine (TETA) for CO_2 capture. Hahn et al. (2016) reported the primary amine, secondary amine, and bibasic amine species functionalized porous SiO_2 and discussed the mechanism of CO_2 adsorption on the SiO_2. Bae (2017) showed that the 3–(2–aminoethylamino) propyldimethoxymetylsilane modified silica can be used as an adsorbent to improve CO_2 capture performance and obtained capture CO_2 capacity of 2.24 mmol/g. The surface of SiO_2 usually has been functionalized with primary and secondary amines for CO_2 capture. Amine modified SiO_2 reacted with CO_2 to form carbamate or bicarbonate species based on the acid–based chemical interaction for improved CO_2 adsorption (Huang et al., 2003). Without the presence of water, the amine groups reacted with CO_2 molecules to create the carbamates group. As another specific, the presence of water impairs this amino group adsorption (Ma et al., 2017). Therefore, the functionalized nano–SiO_2 with water impede is needed to further investigated in future development.

It is difficult to destroy the steady carbon–nitrogen bond of carbamate that is formed in primary amine and secondary amines reaction with CO_2. Also, fascinating tertiary amines as absorbents generate bicarbonates to replace carbamates when tertiary amines reacting with CO_2 (Crooks and Donnellan, 1990; Vaidya and Kenig, 2007) thereby leading to low energy for regeneration of absorbents. Therefore, tertiary amine as an energy saving absorbent is appropriate comparing with primary amines and secondary amines (Gao et al., 2017). Particularly, the rate of primary amines and secondary amines with CO_2 is faster than tertiary amines (Liu et al., 2019a). However, the solubility of CO_2 is higher in tertiary amines solution than one in primary amines and secondary amines solution due to different reaction mechanisms. For example, the reaction molar ratio of tertiary amine and CO_2 is 1:1 to formed bicarbonate structure, while the reaction molar ratio of primary amine or secondary amine and CO_2 is 0.5:1 to formed carbamate structure (Sartorl and Savage, 1983). Tertiary amine can be able to generate a bicarbonate due to no hydrogen on nitrogen when reacted with CO_2 and H_2O, resulting in a better CO_2 adsorption and lower energy depletion for regeneration (Xiao et al., 2016, 2019). Moreover, kinetics is important since it can explain the dynamic adsorption of the sorbent, a lot of kinetic models are applied to the CO_2 adsorption property of tertiary amine (Liu et al., 2019b).

Therefore, this study aimed to develop a sorbent to avert the limits of aqueous amine solutions and take advantage of tertiary amines for CO_2 capture. The tertiary amine loaded nano–SiO_2 was synthesized, and the CO_2 capture performance was studied in the presence of water. The CO_2 adsorption mechanism was investigated by kinetics, and the viscosity of the absorbent dispersion was measured before and after CO_2 adsorption. Finally, tertiary amine functionalized nano–SiO_2 (NS–NR_2) was investigated further in terms of temperature, dispersants, and cycling numbers.

EXPERIMENTAL SECTION

Materials

Methylbenzene(C_7H_8), 3–(trimethoxysilyl)−1−propanamine (KH−540), ethanol (C_2H_5OH), formic acid (HCOOH), formaldehyde (HCHO), hydrochloric acid (HCl), N, N–dimethylformamide (DMF), and sodium hydroxide (NaOH) were purchased from Chengdu Kelong Chemical Reagent Factory (Sichuan, China). Nano–SiO_2 (10–20 nm) was obtained from Aladdin Chemistry Co. (Shanghai, China). All chemical reagents were analytical–grade. CO_2 (g) and N_2 (g) were purchased from Jingli Gas Company (Chengdu, China). Water was double deionized with a Millipore Milli Q system to produce the 18 MM deionized water.

Synthesis and Characterization of Tertiary Amine Functionalized Nano–SiO_2

The nano–SiO_2 loaded with primary amines (NS–NH_2) was prepared first using 3–Aminopropyltrimethoxysilane (KH540) as modifiers, and then it was used as the matrix material to synthesize branched nanomaterials with a tertiary amine group on its surface (NS–NR_2) via methylation of primary amines based on formic acid and formaldehyde. The mechanism is shown in **Figure 1**.

The specific reaction conditions of NS–NH_2, NS–NR_2, and the preparation methods of the nanofluid are shown in **Supplementary Materials**. It is worth noting that add anhydride to promote unreacted primary amine groups undergo acetylation. The optimum reaction conditions of NS–NR_2 are displayed in **Table 1**.

Fourier transform–Infrared (FT–IR) spectra were acquired by the KBr pellet method using a WQF520 spectrometer. Thermogravimetric analysis (TGA) was conducted on a synchronous comprehensive thermal analyzer (Netzsch Scientific Instruments). The microtopography of NS–NR_2 was characterized using an electron microscope (ZEISS Libra 200 FE). The carbon and nitrogen contents were detected by elemental analysis using a Var10EL III instrument. The hydrodynamic diameter and proportion of the nanoparticles were received by a BI 200SM wide-angle dynamic light scattering (DLS) instrument. The rheological property of NS–NR_2 dispersion was measured with a HAAKE MARS III rheometer at 25°C to assess the viscosity.

CO_2 Adsorption and Desorption

NS–NR_2 dispersion was introduced into a gas adsorption bottle. The gas adsorption bottle was put in a constant temperature water bath. The gas flow of CO_2 was controlled at 1 L/min by a gas

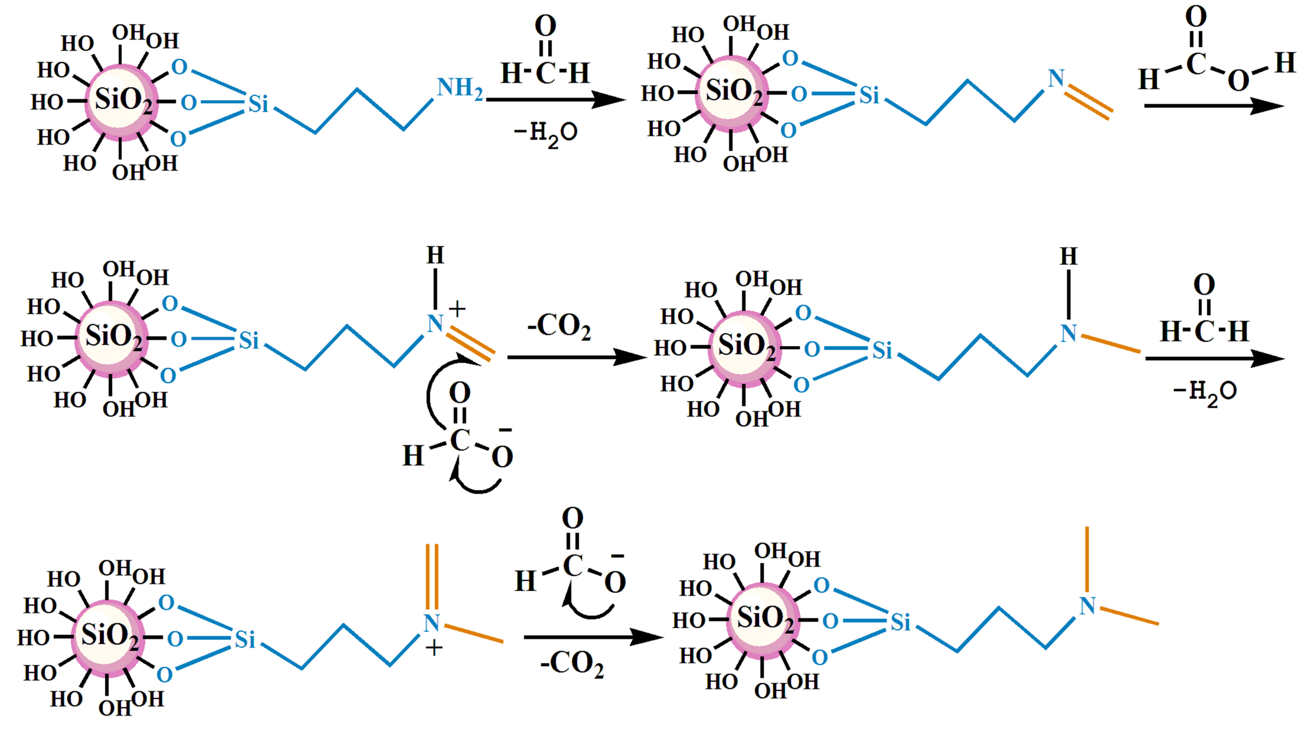

FIGURE 1 | Schematic of the reaction steps of NS–NR_2.

TABLE 1 | Conditions of NS–NR_2.

Time (h)	Temperature (°C)	NS-NH_2: HCOOH: HCHO (g:mol:mol)	Solvent (mL)
12	90	1:6:6	60

flow controller, and CO_2 was bubbling into the high concentrated sulfuric acid to adsorb microscale water in CO_2 gas in a hermetic wild-mouth bottle. After that, the dry CO_2 was flowed through the gas adsorption bottle to reacted with absorbent in the water. The mass change of dispersion was confirmed by an accurate analytical balance (±0.1 mg) until the weight has no change. The amount of adsorption CO_2 on nanoparticles could be calculated under a control test (no nanoparticles). As shown in **Figure S1**, most of the tests were implemented to assure repeatability of the method. The CO_2 adsorption capacity of NS–NR_2 was measured using a gas adsorption system, as shown in **Figure S2**. The CO_2 desorption experiment was simply carried out by bubbling N_2 around 1 L/min instead of injecting CO_2 and keeping the system temperature at 25°C to avoid the huge energy depletion.

The mechanism studies of CO_2 adsorption into NS–NR_2 are often executed using kinetic models including pseudo first order, pseudo second order, and intraparticle diffusion model. The parameter R^2 and relative error (ε) were applied to evaluate the reliability of kinetic models in predicting adsorption capacity, as defined in Equation (1). Based on Equation (1), $q_{e,cal}$ is the predicted date acquired from the model analysis, and $q_{e,exp}$ is the experiment date.

$$\varepsilon(\%) = \frac{q_{ecal} - q_{eexp}}{q_{eexp}} \times 100\% \tag{1}$$

The pseudo first order model that introduced by Langergren in 1898 year (Langergren, 1898) is shown in Equation (2):

$$\log(q_e - q_t) = \log(q_e) - (\frac{k_1}{2.303})t \tag{2}$$

where q_t is the adsorption capacity at a special time, q_e is the adsorption capacity at equilibrium, k_1 is the constant of pseudo first order with a unit of 1/min. The pseudo second order model (Ho and McKay, 1999) is represented by Equations (3) and (4):

$$\frac{t}{q_t} = \frac{1}{k_2 q_e^2} + \frac{t}{q_e} \tag{3}$$

$$h = k_2 \cdot q_e^2 \tag{4}$$

where q_t is the adsorption capacity at a special time, q_e is the adsorption capacity at equilibrium, k_2 is the constant of pseudo second order with a unit of g/mmol min. The intraparticle diffusion model offers the diffusion mechanism of matter in adsorption process as defined in Equation (5):

$$q_t = kt^{1/2} + C \tag{5}$$

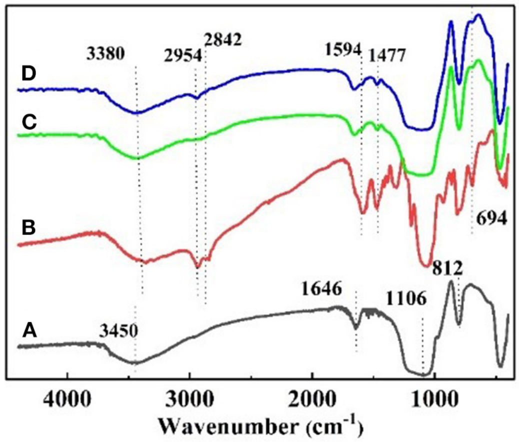

FIGURE 2 | (A) FT–IR spectra of raw SiO$_2$, **(B)** KH540, **(C)** NS–NH$_2$, and **(D)** NS–NR$_2$.

Where q_t is the adsorption capacity at a special time (mmol/g), k is the rate constant of intraparticle diffusion (mmol/g min$^{1/2}$) and C (mmol/g) is as the thickness of the boundary layer; the intercept is positively correlated with the boundary layer. (Hameed et al., 2008; Yousef et al., 2011). Mass transfer of adsorbate to the adsorbent surface (bulk diffusion) and film diffusion into the internal sites (intraparticle diffusion) and other steps occur in the process of adsorption.

RESULTS AND DISCUSSION

Characterization

The FT–IR spectrum of the nanoparticles is shown in **Figure 2**. **Figure 2A** shows the strong adsorption peaks at around 3,450 and 1,646 cm^{-1}, suggest the stretching vibration of the –O–H bonds on the surface of silica. The adsorption peaks near 1,106 and 812 cm^{-1} are the adsorption peaks of the Si–O–Si group, which are characteristic adsorption peaks of SiO$_2$. In the FT–IR spectra of KH540, the adsorption peaks around 3,380 and 1,594 cm^{-1} are the –N–H stretching and NH$_2$ deformation of hydrogen bonded amino groups (Jiao et al., 2015). The adsorption peak at 1,477 cm^{-1} is C–N, and the peaks at 2,954 and 2,842 cm^{-1} are feature adsorption peak of –CH$_3$ and –CH$_2$-, respectively. The peak at 694 cm^{-1} is the adsorption peak of Si–C (Titinchi et al., 2014). In the FT–IR spectra of NS–NH$_2$, the 2,954 cm^{-1} peak of –CH$_3$ disappeared, elucidating that the primary amine was grafted on the surface of SiO$_2$. In **Figure 2D**, the adsorption peak of –CH$_3$ is shown to appear, indicating that –(CH$_2$)$_3$NH$_2$ reacted to –(CH$_2$)$_3$N(CH$_3$)$_2$ on the surface of nano–SiO$_2$.

The microscopic structure of the nanoparticles is shown in **Figure 3** as observed from the TEM morphology. The diameter of NS–NR$_2$ was shown to be approximately 15 nm. The nanoparticles aggregated slightly because of the particle size being in the nanometer scale (Zhao et al., 2014). The evidence from DLS analysis (**Figures 4A,B**) shown the hydrodynamic diameter of NS–NR$_2$ to be approximately 123.6 nm with uniform size distribution. Moreover, it was found that the diameter distribution of nude particles was wider and the agglomeration was more serious than that of the modified nanoparticles.

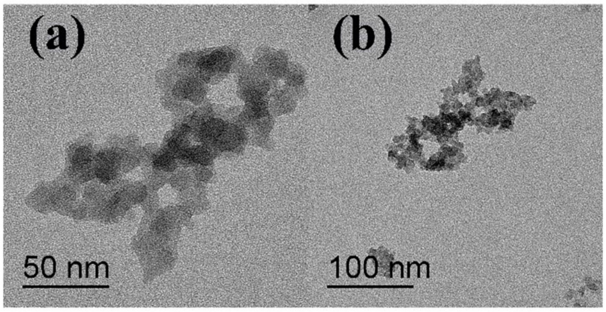

FIGURE 3 | TEM image of NS–NR$_2$ (the scale bars in **a** is 50 nm and **b** is 100 nm).

The element contents of raw SiO$_2$, NS–NH$_2$, and NS–NR$_2$ are shown in **Table 2**. Carbon and nitrogen contents are present in raw SiO$_2$ because many SiO$_2$ materials are often synthesized in an aqueous organic solvent, resulting in remaining carbon and nitrogen in such materials. The contents of carbon and nitrogen for NS–NH$_2$ were shown to be 5.22 and 1.65 mmol/g, respectively, and for NS–NR$_2$ were shown to be 7.14 and 1.39 mmol/g, respectively. The contents of these elements were much higher than raw SiO$_2$. The nitrogen amount in NS–NR$_2$ was lower than that of NS–NH$_2$ because when the molar amount of carbon increases, the molar amount of nitrogen decreases in fixed mass products. The molar ratio of carbon to nitrogen is 3.16, 5.13 in NS–NH$_2$ (SiO$_2$-C$_3$H$_8$N) and NS–NR$_2$ (SiO$_2$-C$_5$H$_{10}$N), respectively. Here, the molar ratio of carbon to nitrogen was adopted to further confirm the grafting of tertiary amines on nano–SiO$_2$.

The successful synthesis of NS–NR$_2$ could also be proved by thermos gravimetric analysis (TGA). Based on the TGA curves in **Figure 5**, the weight retention of raw nano-SiO$_2$, NS–NH$_2$ and NS–NR$_2$ at 900°C under the air atmosphere were 96.86, 89.38, and 87.06%, respectively. For raw nano-SiO$_2$, the mass depletion is attributed to the surface dihydroxylation. In terms of the structure of NS–NH$_2$ and NS–NR$_2$, when the temperature up to 900°C, the primary amine and tertiary amine chains were grafted on the nano-SiO$_2$ has decomposed, respectively. Therefore, compared with the TGA curve of raw nano-SiO$_2$, the surface of nano-SiO$_2$ was modified to primary amine. The different weight loss between in the NS–NH$_2$ and NS–NR$_2$ indicated that tertiary amine was synthesized from primary amine successfully.

CO$_2$ Adsorption and Kinetic Studies

Any amine with a pKa value >5 can react with CO$_2$ in the presence of water (Field and Grolimund, 1988). According to **Figure S3A**, the pH value of NS–NR$_2$ dispersion decreased gradually with the addition of diluted hydrochloric acid (0.01 mol/L). The second derivative of the V$_{\mathrm{HCl}}$-pH curve was obtained (**Figure S3B**), with the zero point of the second

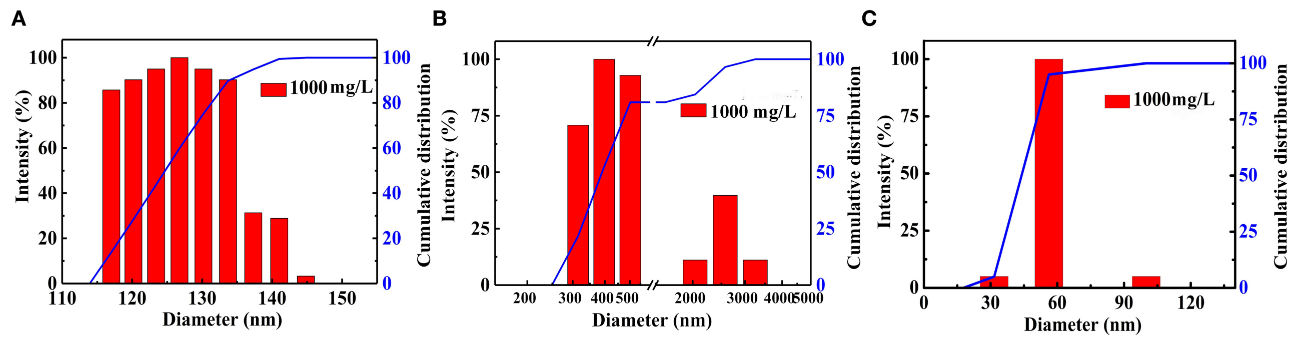

FIGURE 4 | Diameter distribution of **(A)** NS–NR_2 and **(B)** nude nanoparticles in water; **(C)** Diameter distribution of NS–NR_2 in PEG−400 solution (1,000 mg/L).

TABLE 2 | Element contents on nanoparticles.

Sample	C (mmol/g)	N (mmol/g)	Molar ratio of C/N
Raw SiO_2	0.15	0.18	0.85
NS-NH_2	5.22	1.65	3.16
NS-NR_2	7.14	1.39	5.13

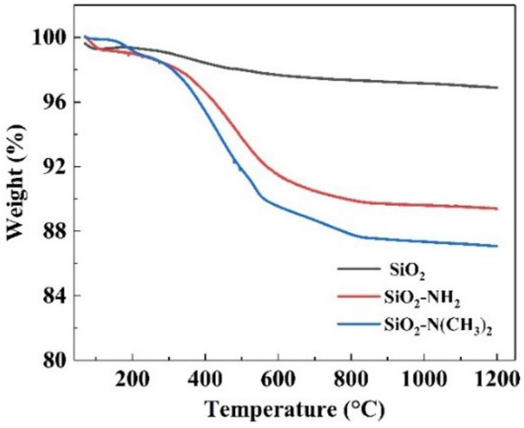

FIGURE 5 | TGA thermograms of raw nano–SiO_2, NS–NH_2, and NS–NR_2.

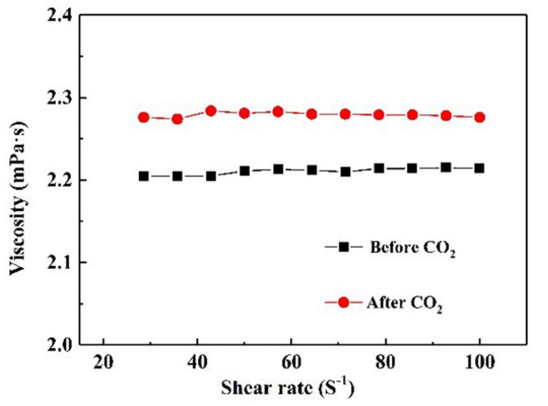

FIGURE 6 | Viscosity of NS–NR_2 dispersion before and after adsorption of CO_2 as a function of shear rate.

derivative corresponding to the extreme point of the curve in **Figure S3A**. As a result, the pKa value was 7.08. The pKa value of 7.08 indicates that NS–NR_2 dispersion can complete adsorption of CO_2. Along with the aeration of CO_2 at 1 L/min, the pH value of NS–NR_2 dispersion dropped rapidly in the first 5 min, after which there were no changes in pH value for 20 min, as shown in **Figure S3C**, which means that NS–NR_2 dispersion (0.1 wt.%) completely saturated CO_2 at 1 L/min CO_2 gas velocity in 20 min.

It is well-known that CO_2 capture is significant influenced by the viscosity of absorbent (Xiao et al., 2019). **Figure 6** demonstrates the rheological property of NS–NR_2 dispersion before and after adsorption CO_2. A rheological plateau in the shear rate region was found for NS–NR_2 dispersion. Before CO_2 adsorption, the nanofluid viscosity was 2.23 mPa·s. After saturation with CO_2, there was a nanofluid viscosity increase to 2.96 mPa·s. This viscosity change is consistent with the ionic liquids in Xiao et al.'s work (Xiao et al., 2019). A possible conclusion is the increase of electrostatic interaction of chains on the NS–NR_2 surface due to CO_2 adsorption (**Figure 7**), resulting in the higher viscosity. However, unlike the high viscosity of ionic liquids, the nanofluid viscosity was very low. The CO_2 capture was not influenced by the increased viscosity.

The CO_2 adsorption capacity of NS–NR_2 was 25 mmol CO_2/g NS–NR_2 in water (0.1 wt.%) at 25°C, as shown in **Table 3**. Compared with other materials (with CO_2 adsorption capacity of 0.1–21.45 mmol/g) (Yu et al., 2012), NS–NR_2 in water has a better CO_2 adsorption capacity.

Kinetic models, such as pseudo first order, pseudo second order, and intraparticle diffusion model, were applied to model the test data. The pseudo first order model is mostly appropriated to describe purely physisorption process without considering the any chemical reaction between CO_2 molecules and sorbent. The pseudo second order model is mostly appropriated to describe purely chemisorption processes with stable chemical bonds between CO_2 molecules and the sorbent. The comparison between the test curves and simulative curves are shown

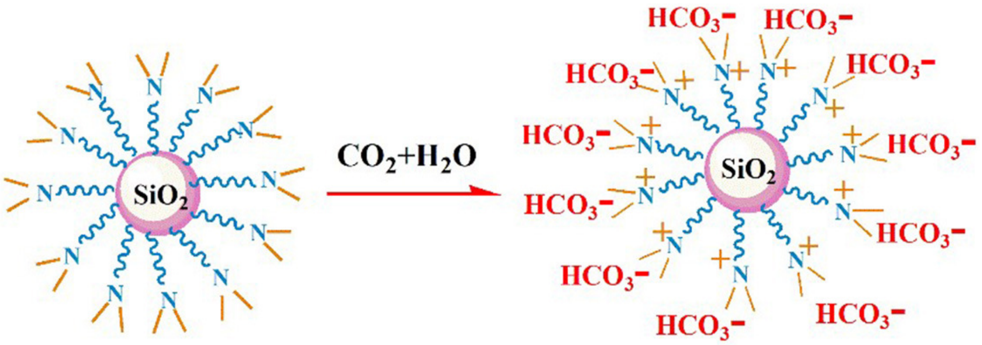

FIGURE 7 | The process for NS–NR$_2$ reacting with CO$_2$.

TABLE 3 | CO$_2$ adsorption of samples at 25°C.

Samples	Volume	CO$_2$ adsorption
Nanofluid (NS-NR$_2$ of 0.06g)	60mL	5.55mmol
Water	60mL	4.05mmol

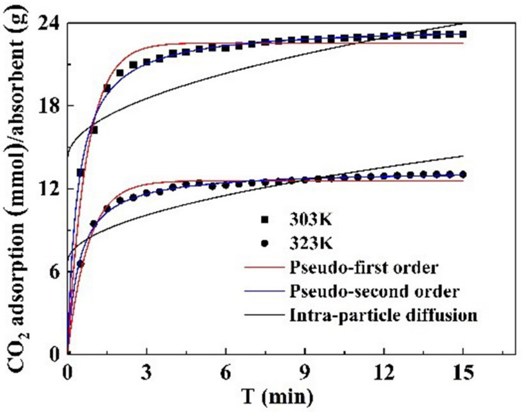

FIGURE 8 | Kinetic plot of CO$_2$ adsorption models at various temperatures.

in **Figure 8**. The model parameters of kinetic at different temperatures and their corresponding coefficients are shown in **Table 4**. The R^2 parameters of pseudo second order and pseudo first order models with experimental data were 0.99 and 0.97, respectively. The relative error for the pseudo second order model, ε, was lower than pseudo first order model. Compared with the R^2, ε parameters, the pseudo second order model was found to fit well with the experiment data. Therefore, chemisorption of CO$_2$ on nanoparticles plays a dominant role in CO$_2$ capture.

The pseudo first order model and pseudo second order model provide interaction insight into the actual mechanism of CO$_2$ adsorption. The surface of the particles is grafted with functional groups to adsorb CO$_2$. This surface adsorption was further verified by the intraparticle diffusion. The model parameters of

TABLE 4 | Kinetic parameters of CO$_2$ adsorption on NS-NR$_2$.

Kinetic model	Parameter	Temperature (°C)	
		30	50
	$q_{e,exp}$ (mmol/g)	23.16	13.03
Pseudo first order	$q_{e,cal}$ (mmol/g)	22.49	12.58
	K_1 (1/min)	3.16	2.84
	R^2	0.9795	0.9777
	Relative error, ε (%)	2.89	3.45
Pseudo second order	$q_{e,cal}$ (mmol/g)	23.82	13.37
	K_2 (g/mmol min)	0.10	0.17
	h (mmol/g min)	56.74	30.39
	R^2	0.9977	0.9963
	Relative error, ε (%)	2.84	2.61
Intra-particles diffusion	K (mmol/g min$^{1/2}$)	2.54	1.99
	C(mmol/g)	14.13	6.64
	R^2	0.5044	0.6011

intraparticle diffusion are revealed in **Table 4**. It is notable that no linear curve can pass through the origin point that is thought to be caused by intraparticle diffusion, suggesting that intraparticle diffusion is not the only factor controlling CO$_2$ adsorption rate at all tested temperatures (Rashidi et al., 2013). Therefore, the adsorption process is not completely controlled by intraparticle diffusion, surface diffusion also plays a role in the whole CO$_2$ adsorption process.

Effect of Some Factors on CO$_2$ Adsorption With NS–NR$_2$

Effect of Temperature

A CO$_2$ capture test was implemented using 0.1 wt.% nanofluid at contrast temperatures of 25, 30, 40, 50, and 60°C, respectively. The CO$_2$ adsorption- temperature curve is revealed in **Figure 9A**. It is obvious that the maximum CO$_2$ loading on the nanoparticles decreased at higher temperatures. Higher temperatures go against CO$_2$ adsorption that is an exothermic reaction. The CO$_2$ adsorption of NS–NR$_2$ compared with that of MSU–J modified with TETA (Jiao et al., 2015) at higher temperatures

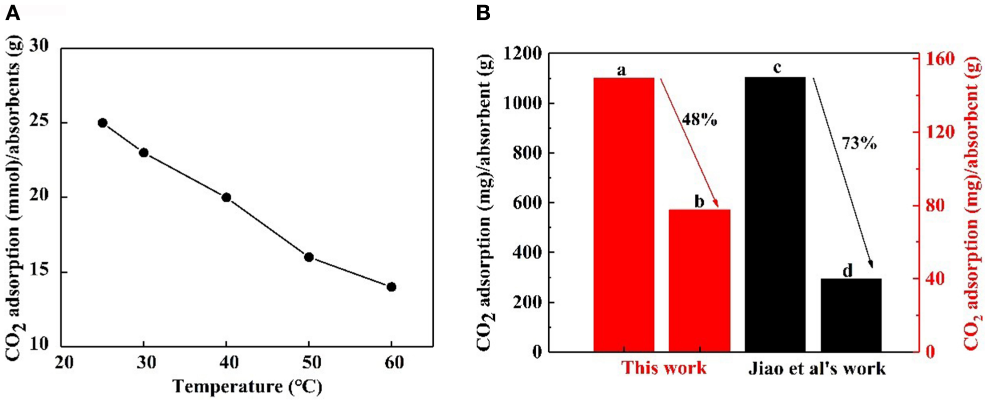

FIGURE 9 | (A) CO_2 adsorption of NS-NR_2 in water at different temperatures. **(B)** CO_2 adsorption of NS–NR_2 at **(A)** 25°C and **(B)** 60°C; CO_2 adsorption of MSU–J at **(C)** 25°C and **(D)**55°C.

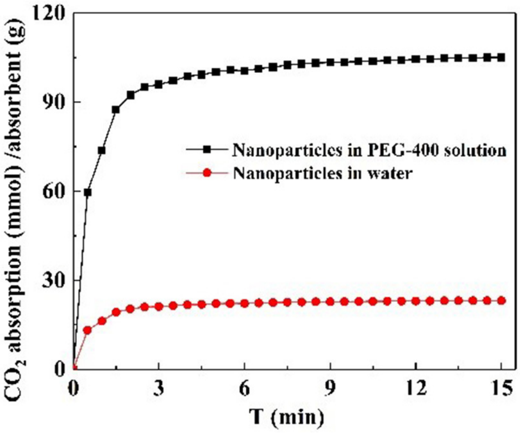

FIGURE 10 | CO_2 adsorption of NS-NR_2 in different dispersants.

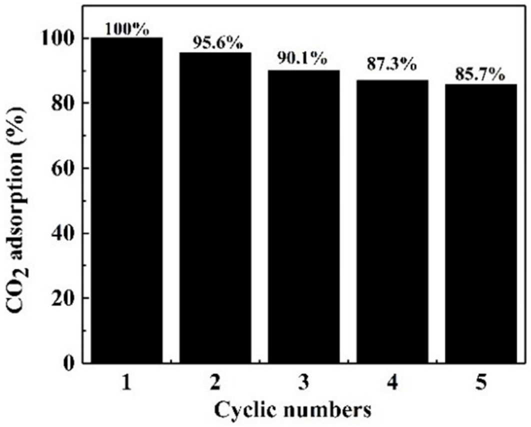

FIGURE 11 | Cyclicity of NS–NR_2 adsorbent in water.

is displayed in **Figure 9B**. The relative comparison presents a view of the advantages of the proposed nanoparticles although a slight difference in the experimental conditions. For the NS–NR_2 absorbent in this work, the CO_2 loading at 60°C decreased to 48% of the CO_2 loading at 25°C, while the CO_2 loading of MSU–J at 55°C decreased to 73% of the CO_2 loading at 25°C. This result can be ascribed to the different mechanisms of CO_2 adsorption. For modified MSU–J absorbent, huge energy was used to generate carbamate group with CO_2. But adsorption of CO_2 loaded nanoparticles enabled bicarbonate formation much easier because of the physical adsorption and chemical adsorption. This result indicates that the NS–NR_2 in this work can capture more CO_2 at higher temperatures.

Effect of Dispersants

CO_2 adsorption capacity in different dispersant agents were investigated. According to the previous test is shown in **Figure S3C**, it was not necessary to perform the experiment for longer than 20 min. Hence, CO_2 adsorption with NS–NR_2 was performed at a temperature of 30°C in different dispersants during this period of 15 min. CO_2 adsorption curves are drawn in **Figure 10**. The maximum CO_2 loading of NS–NR_2 was changed in water or PEG−400 dispersants. The maximum CO_2 loadings of NS–NR_2 in water and PEG−400 solution was 23.16 and 105.34 mmol/g, respectively. This result can be explained by the diameter distribution of nanoparticles, where the diameter distribution in water was 123.6 nm and in PEG−400 solution was 56.7 nm (**Figure 4C**). The tertiary amine groups as specific sites for CO_2 adsorption grafted on the surface of nano–SiO_2 to endow the adsorbents with CO_2 adsorption. Therefore, the more specific sites were exposed on the surface of nanoparticles because of better dispersibility. The dispersibility of nanoparticles is certified by the Derjaguin Landau Verwey Overbeek (DLVO) theory on interparticle interaction potential (Ilyas et al., 2014). The interaction among nanoparticles is caused by electrostatic repulsion and steric resistance in the PEG−400 solution. In addition, using PEG−400 as the dispersant is inexpensive and has lower surfactivity. Surfactants with similar properties can also be used to disperse the nanoparticles for CO_2 capture. Therefore, adding the surfactant improved CO_2 adsorption by enhancing the dispersibility of nanoparticles.

Effect of Cycling Numbers

It is crucial that an absorbent is reusable and retains an efficient CO_2 adsorption capacity (Ma et al., 2017). Therefore, the regeneration tests of the NS–NR_2 absorbent was carried out at 25°C. After CO_2 adsorption in the nanofluid for 20 min, the nanofluid was shifted to CO_2 desorption for regeneration. The CO_2 desorption test was executed for another 20 min by bubbling N_2 around 1 L/min before the absorbent was used for the next round of adsorption. As illustrated in **Figure 11**, five cycles of adsorption were implemented and the initial CO_2 adsorption of absorbent was set as the 100 % baseline. After five cycles, NS–NR_2 adsorbent shown favorable regeneration capacity with a slight decrease of 14.3% in water for NS–NR_2 compared to the initial capacity. The results shown regeneration and efficient CO_2 adsorption capacity of nanoparticles adsorbent. Considering cycling capacity, NS–NR_2 material shows intriguing regeneration ability for CO_2 adsorption.

CONCLUSION

This work synthesized tertiary amino functionalized nano–SiO_2 successfully. The measurements of pKa value and nanofluid viscosity change proved that NS-NR_2 can react with CO_2 in water and nanofluid has a low viscosity. NS–NR_2 shown better CO_2 adsorption capacity, and adsorption kinetics revealed the pseudo second order model was found to fit well with the experiment data. The influence of factors such as temperature, dispersants, and cycling numbers on CO_2 adsorption was investigated. Results indicated higher temperature to work against CO_2 adsorption of NS–NR_2. The CO_2 adsorption performance of NS–NR_2 was greatly promoted because of a better dispersity of nanoparticles with added surfactant. After recycling of absorbent, the NS–NR_2 maintained an efficient CO_2 capture and shown favorable regeneration capacity. The measurements of NS–NR_2 properties on the bases of viscosity, kinetic models, CO_2 capture, and regeneration manifests that NS–NR_2 exhibits satisfying performance to capture CO_2. NS–NR_2 with high CO_2 capture will play a role in storing CO_2 to enhanced oil recovery in CO_2 flooding.

DATA AVAILABILITY STATEMENT

All datasets generated for this study are included in the article/**Supplementary Material**.

AUTHOR CONTRIBUTIONS

NL, QZ, and LT conceived the idea. QZ, WH, TY, and YC implemented the preparation, characterization, and measurement of NS–NR_2. QZ wrote the manuscript. DQ and KC came up with ideas for the manuscript. QZ, LT, and DW discussed and analyzed the experiment data. LT and DW revised the manuscript. NL supervised the whole research work.

FUNDING

This work was supported by the National Natural Science Foundation of China (No. 51674208); Nanchong Science and Technology Project (NC17SY4017); State Key Laboratory of Molecular Engineering of Polymers (Fudan University) (No. K2017-25); PetroChina Innovation Foundation (No. 2018D−5007−0207); Open Foundation of State Key Laboratory of Oil and Gas Geology and Exploitation (Cheng Du University of Technology) (No. PLC20180103); Basic Research Programs of Sichuan Province (No. 2018JY0515); and the Undergraduate Extracurricular Open Experiment of Southwest Petroleum University (KSZ18440, KSZ18441, KSZ18442).

SUPPLEMENTARY MATERIAL

The Supplementary Material for this article can be found online at: https://www.frontiersin.org/articles/10.3389/fchem.2020.00146/full#supplementary-material

REFERENCES

Bae, J. Y. (2017). CO_2 capture by amine-functionalized mesoporous hollow silica. *J. Nanosci. Nanotechno.* 17, 7418–7422. doi: 10.1166/jnn.2017.14778

Benson, S. M., and Orr, F. M. (2011). Carbon dioxide capture and storage. *MRS Bull.* 33, 303–305. doi: 10.1557/mrs2008.63

Bui, M., Adjiman, C. S., Bardow, A., Anthony, E. J., Boston, A., Brown, S., et al. (2018). Carbon capture and storage (CCS): the way forward. *Energy Environ. Sci.* 11, 1062–1176. doi: 10.1039/C7EE02342A

Crooks, J. E., and Donnellan, J. P. (1990). Kinetics of the reaction between carbon dioxide and tertiary amines. *J. Org. Chem.* 55, 1372–1374. doi: 10.1021/jo00291a056

Darunte, L. A., Walton, K. S., Sholl, D. S., and Jones, C. W. (2016). CO_2 capture via adsorption in amine-functionalized sorbents. *Curr. Opin. Chem. Eng.* 12, 82–90. doi: 10.1016/j.coche.2016.03.002

Field, S. M., and Grolimund, K. (1988). Basicity limits for solutes in supercritical fluid chromatography with a carbon dioxide mobile phase. *J. High Res. Chrom.* 11, 727–729. doi: 10.1002/jhrc.1240111010

Gao, H., Xu, B., Han, L., Luo, X., and Liang, Z. (2017). Mass transfer performance and correlations for CO_2 absorption into aqueous blended of DEEA/MEA in a random packed column. *AIChE J.* 63, 3048–3057. doi: 10.1002/aic.15673

Hahn, M. W., Jelic, J., Berger, E., Reuter, K., Jentys, A., and Lercher, J. A. (2016). Role of amine functionality for CO_2 chemisorption on silica. *J. Phys. Chem. B* 120, 1988–1995. doi: 10.1021/acs.jpcb.5b10012

Hameed, B. H., Tan, I. A. W., and Ahmad, A. L. (2008). Adsorption isotherm, kinetic modeling and mechanism of 2,4,6-trichlorophenol on coconut husk-based activated carbon. *Chem. Eng. J.* 144, 235–244. doi: 10.1016/j.cej.2008.01.028

Heydari-Gorji, A., Belmabkhout, Y., and Sayari, A. (2011). Polyethylenimine-impregnated mesoporous silica: effect of amine loading and surface alkyl chains on CO_2 adsorption. *Langmuir* 27, 12411–12416. doi: 10.1021/la202972t

Ho, Y. S., and McKay, G. (1999). Pseudo-second order model for sorption processes. *Process Biochem.* 34, 451–465. doi: 10.1016/S0032-9592(98)00112-5

Huang, H. Y., Yang, R. T., Chinn, D., and Munson, C. L. (2003). Amine-grafted MCM-48 and silica xerogel as superior sorbents for acidic gas removal from natural gas. *Ind. Eng. Chem. Res.* 42, 2427–2433. doi: 10.1021/ie020440u

Ilyas, S. U., Pendyala, R., and Marneni, N. (2014). Preparation, sedimentation, and agglomeration of nanofluids. *Chem. Eng. Technol.* 37, 2011–2021. doi: 10.1002/ceat.201400268

Jiao, J., Cao, J., and Lv, P. P. (2015). Amine-immobilized three-dimensional wormhole mesostructured MSU-J silica for CO_2 adsorption: effect of amine loading and temperature on the adsorption capacity. *Chem. Lett.* 44, 928–930. doi: 10.1246/cl.141151

Kong, X., Li, S., Stromme, M., and Xu, C. (2019). Synthesis of porous organic polymers with tunable amine loadings for CO_2 capture: balanced physisorption and chemisorption. *Nanomaterials* 9:E1020. doi: 10.3390/nano9071020

Lai, N., Li, S., Liu, L., Li, Y., Li, J., and Zhao, M. (2017). Synthesis and rheological property of various modified nano-SiO_2/AM/AA hyperbranched polymers for oil displacement. *Russ. J. Appl. Chem.* 90, 480–491. doi: 10.1134/S1070427217030235

Lai, N., Tang, L., Jia, N., Qiao, D., Chen, J., Wang, Y., et al. (2019). Feasibility study of applying modified nano-SiO_2 hyperbranched copolymers for enhanced oil recovery in low-mid permeability reservoirs. *Polymers.* 11:E1483. doi: 10.3390/polym11091483

Langergren, S. (1898). Zur theorie der sogenannten adsorption gelster stoffe. Kungliga Svenska Vetenskapsakademiens. *Handlingar* 24, 1–39.

Lee, Y., and Park, J. (2015). A review on solid adsorbents for carbon dioxide capture. *J. Ind. Eng. Chem.* 23, 1–11. doi: 10.1016/j.jiec.2014.09.001

Liu, H., Chan, C., Tontiwachwuthikul, P., and Idem, R. (2019a). Analysis of CO_2 equilibrium solubility of seven tertiary amine solvents using thermodynamic and ANN models. *Fuel* 249, 61–72. doi: 10.1016/j.fuel.2019.02.088

Liu, H., Idem, R., and Tontiwachwuthikul, P. (2019b). Novel models for correlation of solubility constant and diffusivity of N_2O in aqueous 1-dimethylamino-2-propanol. *Chem. Eng. Sci.* 203, 86–103. doi: 10.1016/j.ces.2019.03.073

Liu, Y., Huang, N., Yu, Y., Zheng, C., Deng, N., and Liu, J. (2016). Bioactive SiO_2@Ru nanoparticles for osteogenic differentiation of mesenchymal stem cells via activation of Akt signaling pathways. *J. Mater. Chem. B* 4, 4389–4401. doi: 10.1039/C5TB01898F

Ma, Y., Wang, Z., Xu, X., and Wang, J. (2017). Review on porous nanomaterials for adsorption and photocatalytic conversion of CO_2. *Chinese J. Catal.* 38, 1956–1969. doi: 10.1016/S1872-2067(17)62955-3

Rashidi, N. A., Yusup, S., and Hameed, B. H. (2013). Kinetic studies on carbon dioxide capture using lignocellulosic based activated carbon. *Energy* 61, 440–446. doi: 10.1016/j.energy.2013.08.050

Rochelle, G. T. (2009). Amine scrubbing for CO_2 capture. *Science* 325, 1652–1654. doi: 10.1126/science.1176731

Sanz-Perez, E. S., Murdock, C. R., Didas, S. A., and Jones, C. W. (2016). Direct capture of CO_2 from ambient air. *Chem. Rev.* 116, 11840–11876. doi: 10.1021/acs.chemrev.6b00173

Sarkodie, S. A., and Strezov, V. (2019). Effect of foreign direct investments, economic development and energy consumption on greenhouse gas emissions in developing countries. *Sci. Total Environ.* 646, 862–871. doi: 10.1016/j.scitotenv.2018.07.365

Sartorl, G., and Savage, D. W. (1983). Sterically hindered amines for CO_2 removal from gases. *Ind. Eng. Chem. Fundam.* 22, 239–249. doi: 10.1021/i100010a016

Titinchi, S. J. J., Piet, M., Abbo, H. S., Bolland, O., and Schwieger, W. (2014). Chemically modified solid adsorbents for CO_2 capture. *Energy Proc.* 63, 8153–8160. doi: 10.1016/j.egypro.2015.12.337

Vaidya, P. D., and Kenig, E. Y. (2007). CO_2-alkanolamine reaction kinetics: a review of recent studies. *Chem. Eng. Technol.* 30, 1467–1474. doi: 10.1002/ceat.200700268

Wang, F., Gao, S., Pan, J., Li, X., and Liu, J. (2019). Short-chain modified SiO_2 with high absorption of organic PCM for thermal protection. *Nanomaterials* 9:E657. doi: 10.3390/nano9040657

Xiao, M., Liu, H., Gao, H., Olson, W., and Liang, Z. (2019). CO_2 capture with hybrid absorbents of low viscosity imidazolium-based ionic liquids and amine. *Appl. Energy* 235, 311–319. doi: 10.1016/j.apenergy.2018.10.103

Xiao, M., Liu, H., Idem, R., Tontiwachwuthikul, P., and Liang, Z. (2016). A study of structure–activity relationships of commercial tertiary amines for post-combustion CO_2 capture. *Appl. Energy* 184, 219–229. doi: 10.1016/j.apenergy.2016.10.006

Yousef, I., ElEswed, B., and AlMuhtaseb, A. A. H. (2011). Adsorption characteristics of natural zeolites as solid adsorbents for phenol removal from aqueous solutions: kinetics, mechanism, and thermodynamics studies. *Chem. Eng. J.* 171, 1143–1149. doi: 10.1016/j.cej.2011.05.012

Yu, C. H., Huang, C. H., and Tan, C. S. (2012). A review of CO_2 capture by absorption and adsorption. *Aerosol Air Qual. Res.* 12, 745–769. doi: 10.4209/aaqr.2012.05.0132

Zhao, Y., Pan, Y., Nitin, N., and Tikekar, R. V. (2014). Enhanced stability of curcumin in colloidosomes stabilized by silica aggregates. *LWT Food Sci. Technol.* 58, 667–671. doi: 10.1016/j.lwt.2014.03.017

Conflict of Interest: DQ was employed by the Engineer Technology Research Institute, CNPC Xibu Drilling Engineering Company Limited company.

The remaining authors declare that the research was conducted in the absence of any commercial or financial relationships that could be construed as a potential conflict of interest.